

## Shear-induced structural transition in a lyotropic lamellar phase studied using small angle neutron and light scattering

T Kato<sup>1,3</sup>, K Miyazaki<sup>1</sup>, Y Kawabata<sup>1</sup>, S Komura<sup>1</sup>, M Fujii<sup>1</sup> and M Imai<sup>2</sup>

<sup>1</sup> Department of Chemistry, Tokyo Metropolitan University, Hachioji, Tokyo 192-0397, Japan

<sup>2</sup> Department of Physics, Ochanomizu University, Bunkyo, Tokyo 112-0012, Japan

E-mail: kato-tadashi@c.metro-u.ac.jp

Received 30 December 2004, in final form 14 February 2005

Published 22 July 2005

Online at [stacks.iop.org/JPhysCM/17/S2923](http://stacks.iop.org/JPhysCM/17/S2923)

### Abstract

We study the effects of shear flow on structures of the lamellar phase formed in a nonionic surfactant C<sub>16</sub>E<sub>7</sub> (hepta(oxyethylene glycol)-*n*-hexadecylether)/D<sub>2</sub>O system by using small angle neutron scattering (SANS) and small angle light scattering (SALS) in the range of shear rate 10<sup>-3</sup>–30 s<sup>-1</sup>. As the shear rate increases from 0.3 to 1 s<sup>-1</sup>, the lamellar repeat distance for the 48 wt% sample is decreased significantly and discontinuously. With further increase in the shear rate, *d* increases through a sharp minimum at 1 s<sup>-1</sup>. The minimum value does not depend on the surfactant concentration very much and is nearly equal to the thickness of the bilayers. At this shear rate (1 s<sup>-1</sup>), the intensity of the polarized SALS is strongly enhanced in the small angle region in the vorticity direction. These results suggest that water layers are excluded by shear flow and that large concentration fluctuations on the μm scale are induced, which corresponds to local segregation into two regions; one of these has concentrated lamellar structures and the other is a water-rich region. As the shear rate increases further (to 3 s<sup>-1</sup>), a broad diffraction peak appears in the vorticity direction in the polarized SALS whereas a four-lobe pattern is observed in the depolarized SALS. These results, together with the two-dimensional SANS pattern, suggest the formation of close-packed onions elongated along the flow direction at 3 s<sup>-1</sup>. Comparison is made with the study of Nettekheim *et al* (2003 *Langmuir* **19** 3618) who report the formation of multilamellar cylinders as intermediate structures, between lamellae and spherical onions.

<sup>3</sup> Author to whom any correspondence should be addressed.

## 1. Introduction

It is well known that shear flow induces structural changes in materials when the product  $\dot{\gamma}\tau$  is larger than unity, where  $\dot{\gamma}$  is the shear rate and  $\tau$  is the specific timescale of fluctuations of these structures. For surfactant self-assembly, this condition is easily satisfied because  $\tau$  can be of the order of  $10^{-9}$ – $10^2$  s whereas experimentally available shear rates are less than  $10^4$  s $^{-1}$ . In the past ten years, effects of shear flow have been studied extensively by using microscopy, NMR, and various kinds of scattering techniques. Among them, the lamellar phase has become of interest because the shear-induced state is sometimes not related to an existing equilibrium. Roux and co-workers [1–4] have found transformation from the lamellar phase to the ‘onion phase’ where multilamellar vesicles are close packed. They have also found a transition from ‘state II’ (the isotropic state of onions, the disordered state) to ‘state III’ (the oriented state of lamellae) as well as to ‘state IV’ (small onions in compact planes, the ordered state) and from state IV to ‘state V’ (big onions in compact planes, the ordered phase). Following their work, various kinds of shear effects have been reported: change in orientation of membranes [5, 6], sponge-to-lamellar transformation [7, 8], multilamellar-to-unilamellar vesicle transformation [9], reduction in the spacing [10–14], collapse of membranes [15], and formation of multilamellar cylinders or deformed onions [16–19]. It should be noted that these studies have been performed for the shear rates of  $1$ – $5 \times 10^3$  s $^{-1}$ .

Recently, we have measured small angle neutron scattering (SANS) under shear flow for the lamellar phase of the C<sub>16</sub>E<sub>7</sub> (hepta(oxyethylene glycol)-*n*-hexadecylether)/water system (40–55 wt% of C<sub>16</sub>E<sub>7</sub>) at 70 °C, paying attention to the structural change in the relatively low shear rate range,  $10^{-3}$ – $30$  s $^{-1}$  [20]. When the shear rate increases from 0.1 to 1 s $^{-1}$ , the repeat distance ( $d$ ) is decreased significantly (down to about 40% of  $d$  at rest in the most significant case) and discontinuously. With further increase in the shear rate,  $d$  increases through a sharp minimum. This, together with other results, strongly suggests that water layers are excluded by shear flow and that the lamellar phase segregates into two regions; one of these has concentrated lamellar structures and the other is a water-rich region. However, macroscopic phase separation is not observed by the naked eye.

In the present study, we measure polarized and depolarized small angle light scattering (SALS) to confirm the above prediction from the SANS results on the nm scale and to provide a basis for discussing the structural transition on the  $\mu$ m scale. Preliminary results for the unpolarized mode in SALS have been reported elsewhere [21].

## 2. Experimental details

A rheometer (Nihon Rheology Kiki, NRM-2000) was modified for SALS measurements under shear flow. The sample cell is almost the same as that for the SANS measurements: a Couette-type shear cell consisting of two concentric cylinders made of quartz. The stator diameter and the gap are 48 and 1 mm, respectively. The temperature of the cell is controlled to  $\pm 0.1$  °C by Peltier elements and a heater in an air bath. To prevent sample evaporation, a vapour seal is incorporated in the cell. A He–Ne laser beam (NEC GLG5360, 5 mW at 632.8 nm), which is polarized horizontally, is passed down the velocity gradient axis of the Couette cell (corresponding to the so-called radial configuration) and through an analyser. The intensity of scattered light is detected by a CCD camera system (Hamamatsu Photonics C4880-80-22A). A schematic presentation of the shear SALS apparatus has been reported previously [21]. In the present study, we measure both polarized ( $H_h$ ) and depolarized ( $V_h$ ) scatterings where the analyser is set parallel and perpendicular, respectively, to the incident polarization. The details of the apparatus will be presented elsewhere [22].

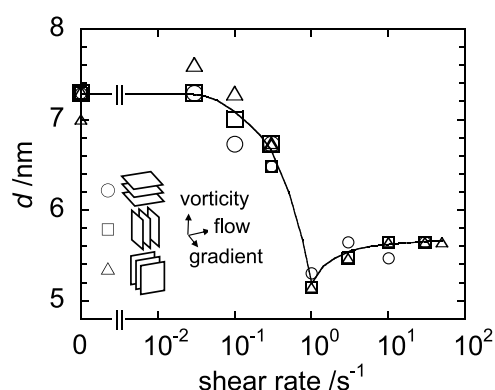


**Figure 1.** Shear rate dependence of the repeat distance for the vorticity (O), transverse (□), and parallel (Δ) orientations previously reported [20]. The different symbol sizes correspond to different runs.

SALS measurements have been performed for the 48 wt% sample at 70 °C. The shear history of the sample is almost the same as that for the previous SANS measurements at 48 wt% [20]; the shear rate has been changed in the order 0.3 s<sup>-1</sup> (2 h), 1 s<sup>-1</sup> (2 h), and 3 s<sup>-1</sup> (1 h).

### 3. Results and discussion

Figure 1 shows shear rate dependence of the repeat distance at 48 wt% obtained by SANS measurements, which has been previously reported [20]. For the lamellar structure, there are three principal orientations, perpendicular, transverse, and parallel orientations, with the layer normal along the vorticity, flow, and velocity gradient directions, respectively. These three orientations can be detected by using two kinds of configurations; one is the so-called radial configuration where the beam is directed through the centre of the cell (along the velocity gradient direction), and the other is the tangential configuration where the beam is directed through the end of the cell (along the flow direction). The different symbols in figure 1 correspond to the different orientations of lamellae. In the range 0–0.03 s<sup>-1</sup>, the repeat distance is almost independent of the shear rate. As the shear rate increases from 0.3 to 1 s<sup>-1</sup>,  $d$  is reduced suddenly from 6.6 to 5.2 nm. With the further increase in the shear rate,  $d$  increases again through a minimum (referred to as  $d^*$ , hereafter). This figure also demonstrates that such a specific shear rate dependence of  $d$  is obtained for all the principal orientations of lamellae. Similar shear rate dependences have been obtained for other concentrations. As the concentration of C<sub>16</sub>E<sub>7</sub> decreases from 55 to 40 wt%,  $d$  increases from 6.5 to 8.5 nm at rest whereas  $d^*$  remains almost constant (~5 nm) and nearly equal to the thickness of the bilayers at rest obtained from the line shape analysis of small angle x-ray scattering [23]. These results strongly suggest that water layers are excluded by shear flow and that the lamellar phase segregates into surfactant-rich and water-rich regions.

Theoretical prediction of the shear-induced collapse has been reported by Bruinsma and Rabin [24] and Ramaswamy [25]. According to these theories, the critical shear rate above which the collapse occurs can be expressed in terms of the interlayer spacing ( $d$ ), the viscosity of the solvent ( $\eta$ ), and the bending constant of a surfactant layer ( $\kappa$ ). For  $\eta \sim 1 \text{ cp} = 10^{-3} \text{ Pa s}$ ,  $d \sim 10 \text{ nm}$ , and  $\kappa \sim k_B T$ , the critical shear rate is calculated to be 10<sup>6</sup> s<sup>-1</sup> which is more than six orders of magnitude higher than the shear rate giving  $d^*$  in the present study. It should be

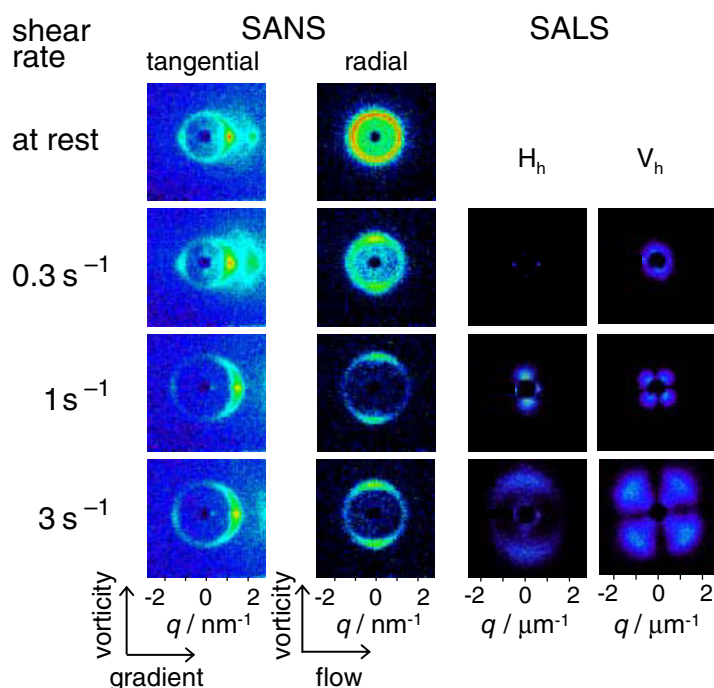


**Figure 2.** Evolutions of 2D patterns of SANS [20] and polarized ( $H_h$ ) and depolarized ( $V_h$ ) SALS with increasing shear rate, from 0 to  $3 \text{ s}^{-1}$ . No significant scattering pattern is observed at rest for SALS.

(This figure is in colour only in the electronic version)

noted that these theories assume direct suppression of undulation fluctuations of membranes by shear flow. In this case, the reduction of  $d$  should be observed only for a limited orientation (probably the parallel orientation). In the present study, however, the shear rate dependences of  $d$  are almost the same for all the principal directions, as can be seen from figure 1.

Figure 2 shows evolutions of 2D (two-dimensional) SALS patterns with increasing shear rate for  $H_h$  (polarized) and  $V_h$  (depolarized) scattering. For comparison, previously reported SANS patterns for both tangential and radial configurations are also included. The SANS pattern at rest for the radial configuration demonstrates that the orientations of the lamellae are isotropic in the vorticity–flow plane. In the vorticity–velocity gradient plane, on the other hand, the lamellae are oriented in the parallel direction, as can be seen from the pattern for the tangential configuration. So the contributions of the three principal orientations are in the following order: parallel > perpendicular  $\sim$  transverse.

The 2D SALS data in figure 2 were reduced to 1D (one-dimensional) data in the vorticity directions by integrating the scattering intensity over a segment of width  $\Delta\phi = \pm 10^\circ$  where  $\phi$  is the azimuthal angle. The 1D patterns obtained for  $H_h$  and  $V_h$  scattering are shown in figures 3(a) and (b), respectively. For the shear rate of  $1 \text{ s}^{-1}$  where the repeat distance takes a minimum, the  $H_h$  scattering intensity in the small angle region is strongly enhanced. This indicates large concentration fluctuations on the  $\mu\text{m}$  scale and is therefore consistent with the prediction from the SANS results on the nm scale. As the shear rate increases up to  $3 \text{ s}^{-1}$ , a broad diffraction peak appears along the vorticity direction, indicating that some sort of regular structure is formed. The repeat distance calculated from the peak position is about  $3.8 \mu\text{m}$ .

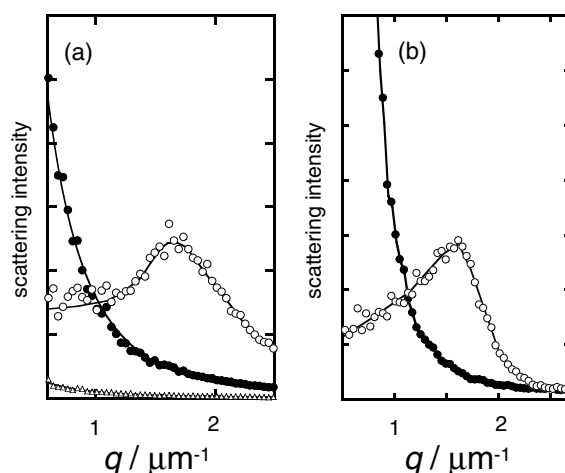


**Figure 3.** 1D polarized ( $H_h$ ) and depolarized ( $V_h$ ) SALS patterns for the shear rates of  $0.3 \text{ s}^{-1}$  ( $\Delta$ ),  $1 \text{ s}^{-1}$  ( $\bullet$ ), and  $3 \text{ s}^{-1}$  ( $\circ$ ) obtained by integrating the 2D scattering intensity over a segment of width  $\Delta\phi = \pm 10^\circ$  where  $\phi$  is the azimuthal angle.

In the  $V_h$  scattering, on the other hand, a four-lobe pattern is observed at  $3 \text{ s}^{-1}$ . It is well known that such a four-lobe pattern is observed for optically anisotropic spheres like polymer spherulites [26, 27]. The radius of the anisotropic sphere ( $R$ ) is calculated to be about  $5.0 \mu\text{m}$  from the observed peak position ( $q_{\text{max}}$ ) of the 1D  $V_h$  scattering pattern using the relation  $q_{\text{max}}R = 4.09$  [26, 27]. In surfactant systems, a multilamellar vesicle (or onions) may be the most probable candidate, as already reported for several systems [1–4, 16–19]. However, spherical onions are inconsistent with the SANS results; the 2D pattern shows a pronounced diffraction peak in the vorticity direction (see figure 2), which indicates that the perpendicular orientation (the normal vector of the lamellae is along the vorticity direction) dominates. If the onions are elongated along the flow direction, on the other hand, the experimental results can be explained because only their hemispherical parts contribute to the four-lobe pattern in the SALS and because the cylindrical part gives a diffraction peak in the vorticity direction in the SANS. It should be noted that the SANS pattern in the tangential configuration indicates that the parallel orientation (the normal vector of the lamellae is along the velocity gradient direction) dominates compared to the perpendicular orientation (see figure 2). Therefore, the cross section perpendicular to the flow direction may be not circular but elongated along the vorticity direction.

Nettesheim *et al* [19] have reported a shear-induced transition from a lamellar phase to multilamellar vesicles using SANS and SALS for 40 wt% samples of  $\text{C}_{10}\text{E}_3$  and  $\text{C}_{12}\text{E}_4$  in  $\text{D}_2\text{O}$  in the shear rate range  $1\text{--}100 \text{ s}^{-1}$ . They have found that there is the formation of an intermediate structure oriented in the flow direction, corresponding to long, multilamellar cylinders (or deformed onions) before the formation of spherical onions. According to their results, however, the four-lobe pattern is observed in the SALS only for the shear rate where the SANS gives an isotropic 2D pattern<sup>4</sup>. Moreover, the repeat distance remains constant throughout the transition process (lamellar  $\rightarrow$  multilamellar cylinders  $\rightarrow$  onions). In the present study, on the other hand, the four-lobe pattern in the SALS and the anisotropic SANS

<sup>4</sup> In [16, 17], the four-lobe pattern in the depolarized SALS and the anisotropic SANS patterns have been observed at the same shear rate. In these studies, however, they demonstrate that spherical onions already formed at low shear rates become deformed when the shear rate increases further.

pattern have been observed at the same shear rate ( $3 \text{ s}^{-1}$ ) and the repeat distance is decreased significantly, as previously described. Nettesheim *et al* have also shown that the transition from lamellae to multilamellar cylinders is controlled by the shear stress. For the systems  $\text{C}_{10}\text{E}_3$  and  $\text{C}_{12}\text{E}_4$  in  $\text{D}_2\text{O}$ , the transition occurs at the shear stress 40–100 Pa. In our system, on the other hand, the shear stress in the steady state is less than  $1.5 \text{ Pa}$  above  $1 \text{ s}^{-1}$  [28], which is much lower than their results.

Although theoretical studies of the transition from the lamellar phase to the onion phase have been reported by several workers [2, 29, 30], the transition mechanism is still unclear. The present results suggest that the local segregation may play an important role in the transition processes.

### Acknowledgment

This research was partially supported by the Ministry of Education, Science, Sports and Culture, Grant-in-Aid for Scientific Research (B), 15340140, 2003.

### References

- [1] Roux D 2000 *Nonequilibrium Dynamics, Metastability and Flow* ed M Cates, M R Evans and P Osborne (Bristol: Institute of Physics Publishing) chapter 7
- [2] Diat O, Roux D and Nallet F 1993 *J. Physique* **3** 1427
- [3] Diat O, Roux D and Nallet F 1995 *Phys. Rev. E* **51** 3296
- [4] Sierro P and Roux D 1997 *Phys. Rev. Lett.* **78** 1496
- [5] Penfold J, Staples E, Lodhi A, Tucker K I and Tiddy G J T 1997 *J. Phys. Chem. B* **101** 66
- [6] Berghausen J, Zipfel J, Berghausen J, Lindner P and Richtering W 1998 *Europhys. Lett.* **43** 683
- [7] Yamamoto J and Tanaka H 1996 *Phys. Rev. Lett.* **77** 4390
- [8] Leon A, Bonn D, Meunier J, Al-Kahwaji A and Kellay H 2001 *Phys. Rev. Lett.* **86** 938
- [9] Bergmeier M, Gradzielski M, Hoffmann H and Mortensen K 1998 *J. Phys. Chem. B* **102** 2837
- [10] Yamamoto J and Tanaka H 1995 *Phys. Rev. Lett.* **74** 932
- [11] Minewaki K, Kato T, Yoshida H and Imai M 1999 *J. Therm. Anal. Calorimetry* **57** 753
- [12] Minewaki K, Kato T and Imai M 2001 *Stud. Surf. Sci. Catal.* **132** 185
- [13] Imai M, Nakaya K and Kato T 2001 *Eur. Phys. J. E* **5** 391
- [14] Idziak S H J, Welch S E, Kisilak M, Mugford C, Potvin G, Veldhuis L and Sirota W B 2001 *Eur. Phys. J. E* **6** 139
- [15] Al-Kahwaji A and Kellay H 2000 *Phys. Rev. Lett.* **84** 3073
- [16] Weigel R, Lauger J, Richtering W and Lindner P 1996 *J. Physique* **6** 529
- [17] Zipfel J, Richtering W and Lindner P 1998 *Physica B* **241–243** 1002
- [18] Zipfel J, Nettesheim F, Lindner P, Le T D, Olsson U and Richtering W 2001 *Europhys. Lett.* **53** 335
- [19] Nettesheim F, Zipfel J, Olsson U, Renth F, Linder P and Richtering W 2003 *Langmuir* **19** 3618
- [20] Kato T, Minewaki K, Kawabata Y, Imai M and Takahashi Y 2004 *Langmuir* **20** 3504
- [21] Kato T, Minewaki K, Miyazaki K, Kawabata Y, Shikata T, Komura S and Fujii M 2004 *Prog. Colloid Polym. Sci.* **129** 9
- [22] Miyazaki K, Kawabata Y and Kato T 2005 unpublished
- [23] Minewaki K, Kato T, Yoshida H, Imai M and Ito K 2001 *Langmuir* **17** 1864
- [24] Bruinsma R F and Rabin Y 1992 *Phys. Rev. A* **45** 994
- [25] Ramaswamy S 1992 *Phys. Rev. Lett.* **69** 112
- [26] Stein R S and Rhodes M B 1960 *J. Appl. Phys.* **31** 1873
- [27] Samuels R J 1971 *J. Polym. Sci. A* **9** 2165
- [28] Miyazaki K, Kosaka Y, Kawabata Y and Kato T 2005 unpublished
- [29] Zilman A G and Granek R 1999 *Eur. Phys. J. B* **11** 593
- [30] Mallow S and Olmsted P D 2002 *Eur. Phys. J. E* **8** 485